Cell Structure Evolution and the Crystallization Behavior of Polypropylene/Clay Nanocomposites Foams Blown in Continuous Extrusion

ARTICLE *in* INDUSTRIAL & ENGINEERING CHEMISTRY RESEARCH · SEPTEMBER 2010

Impact Factor: 2.59 · DOI: 10.1021/ie101225f

4 AUTHORS, INCLUDING:

Wentao Zhai
Chinese Academy of Sciences
62 PUBLICATIONS **973** CITATIONS
SEE PROFILE

C.B. Park
University of Toronto
540 PUBLICATIONS **6,988** CITATIONS
SEE PROFILE

Cell Structure Evolution and the Crystallization Behavior of Polypropylene/Clay Nanocomposites Foams Blown in Continuous Extrusion

Wentao Zhai, Takashi Kuboki, Lilac Wang, and Chul B. Park*

Microcellular Plastics Manufacturing Laboratory, Department of Mechanical and Industrial Engineering, University of Toronto, Toronto, Ontario, M5S 3G8 Canada

Eung K. Lee and Hani E. Naguib

Department of Materials Science and Engineering, University of Toronto, Toronto, Ontario, M5S 3G8 Canada

In this study, linear homopolypropylene/clay (HPPC) nanocomposite foams with a high expansion ratio of about 18 and a high cell density of about 1.7×10^8 cells/cm^3 were produced using an extrusion foaming method with CO_2 as the physical blowing agent. The result was much better than pure HPP foams with expansion ratios of 1.7−2.2 and cell densities of 10^3-10^5 cells/cm^3 obtained even at the same foaming conditions. The nanoclays had a half-exfoliated structure in the HPP matrix, and their presence dramatically affected the viscoelastic properties of HPP melt and foaming behaviors. It was found that the introduction of a small amount of nanoclay significantly increased the cell morphology of HPP foams at low die temperatures, where the cell wall was very thin and cell distribution was uniform. With an increase in nanoclay content of up to 5 wt %, cell morphology was improved gradually at broader die temperatures. Based on the cell morphology results, a suitable foaming window for clay content and die temperature was established. The mechanisms behind these phenomena are discussed from the perspective of cell nucleation and coalescence. Microstructures were found in the cell walls of HPP and HPPC nanocomposite foams, and they tended to evolve with cell wall thickness, depending on the die temperatures. Scanning electron microscopy (SEM) observation of foams and solvent-etched foams revealed that the microstructures in the cell walls were formed by covering large-sized crystals and that the absence of microstructures was due to the presence of small-sized crystals in the cell walls. A distribution of crystal sizes was observed across the foamed samples, which was affected by the die temperature and the introduction of nanoclay. The possible reasons were elaborated by considerations of temperature gradient. DSC tests indicated that the foaming process induced a low-temperature peak (T_{m1}) and its heat of fusion (ΔH_{m1}) tended to evolve with the die temperature and the introduction of nanoclay.

Introduction

Polypropylene (PP) has many desirable and beneficial properties, such as a high melting point, a high tensile modulus, low density, excellent chemical resistance, and easy recycling.[1] These outstanding properties and a low material cost have made linear PP foams a potential substitute for other thermoplastic foams, such as polyethylene (PE) and polystyrene (PS) in various industrial applications.[2] Owing to the weak melt strength and melt elasticity, however, the fabrication of linear PP foams has not been successful. It was found that the cell walls are not strong enough to bear any extensional force during bubble growth and that the bubbles are prone to coalesce and collapse during foam processing. Consequently, foamed PP products usually have a high open-cell content and nonuniform cell distribution[3−5] and thus are not good for practical applications.

To compensate for PP's weak melt strength, different methods have been proposed to improve its linear foamability, such as long-chain branching,[6−9] cross-linking,[5,10−13] polymer blending, and compounding.[14−20] For example, several companies have developed commercial branched PP resins for the production of good PP foams. However, there are cost challenges to wide use, as branched PP resin costs at least twice as much as linear PP. Blending with PE has been used to improve the cell morphology of PP foam,[21−24] but the ability of PE to do so seems limited. Furthermore, it is difficult to produce PP foams with a high expansion ratio if only linear PP is used. Blending with branched PP has been verified as an effective method for producing low-density PP foam, and the addition of 25% high-melt-strength PP was found to significantly improve the cell morphology and expansion ratio of linear PP foams.[25] Currently, the introduction of nanoclay has attracted attention for improving PP's foaming behavior.[16−18,26]

Nanoclay particles have a platelet-like shape and are composed of layers that are almost 1−2 nm thick. The high aspect ratio and large surface area of nanoclay particles potentially offer good reinforcing efficiency and improved dimensional and thermal stability. Well-dispersed nanoclay is one kind of nucleating agent that can reduce the energy barrier of cell nucleation by inducing a local stress variation in polymer/gas solutions[27] and can thus enhance cell nucleation and increase cell density significantly. This phenomenon has been observed in various polymer/filler nanocomposite foaming systems, such as PE/clay,[28−30] PS/clay,[31−33] nylon/clay,[34−36] and polycarbonate (PC)/SiO_2.[37] Introduction of nanoparticles can also increase the polymer's melt strength or induce strain hardening in the melt. It was found that PP melt exhibited an obvious strain hardening with the introduction of well-dispersed nanoclay accompanied by an orientation of clay platelet along the flow direction.[38−40] A similar phenomenon was observed in PEEK/carbon nanofiber composite,[19] where the melt strength of PEEK increased significantly upon the addition of carbon nanofiber

* To whom correspondence should be addressed. E-mail: park@mie.utoronto.ca.

10.1021/ie101225f
Published on Web 09/17/2010

and resulted in the dramatically improved cell morphology of foam products. The cell growth process is a biaxial extension to the cell wall in nature.[41] This action is usually associated with nanoparticle orientation and the increase in extensional viscosity that facilitates the stability of cell structure and the reduction of cell coalescence during foam processing.[16] The batch method has been used often by researchers to study the effects of nanofillers on polymeric foaming. However, considering the high commercial production rate requirement, a continuous foaming process is now becoming popular. In this study, a single extruder system was used to foam PP and PP/clay nanocomposites and to reveal the effects on the foaming behavior of PP of the introduction of nanoclay.

Polymer crystallization is a general phenomenon and a very important process because it controls the polymer's structural formation and, thereby, strongly influences the final product's properties.[42] It has been shown that supercritical CO_2 can swell and plasticize polymers, which increases the mobility of the polymer chains and, hence, allows for a fast relaxation, subsequently resulting in rapid polymer crystallization.[43,44] At the same time, the presence of supercritical CO_2 has been verified to induce the transition of crystal form in polymers.[45] For such polymers as PP with a high crystallization rate, a study using high-pressure differential scanning calorimetry (HPDSC) indicated that the presence of high-pressure CO_2 tended to decrease PP's crystallization temperature.[46] In the extrusion foaming process, foam crystallization takes place under very special situations: The polymer melt is stretched, there is a significant cooling effect during gas depressurization, the cell wall surfaces are in contact with the colder blowing agent, and the thickness of each wall is in the micrometer range.[47] Consequently, the polymer's crystallization behavior in this situation is very different from that at atmospheric pressure, and hence, it is expected to affect the properties of polymeric foams to some degree. However, only limited research has been done on this topic.[47]

A linear PP homopolymer (i.e., homopolypropylene, HPP) with a high melt flow index was selected in this study. An HPP/clay nanocomposite master batch with a clay content of 5 wt % was prepared first with a twin-screw extruder, and then a series of composites with various clay contents were obtained by diluting the master batch with HPP. X-ray diffraction (XRD) was used to characterize the dispersion of nanoclay in the PP matrix. Using the extrusion method, HPP and HPPC nanocomposites were foamed with 5 wt % CO_2 as the physical blowing agent, and the foamed samples were obtained from high to low die temperatures. In this study, the evolution of the cell structures of HPP and HPPC nanocomposite foams in relation to the die temperature and nanoclay content was studied. Then, a map of a suitable foaming window was established. Based on the cell density and melt viscosity data, mechanisms of how nanoclay introduction affects HPP foaming behavior were studied. It was seen that some microstructures were present in the cell walls and were then absent under some conditions independent of whether nanoclay was introduced. Scanning electron microscopy (SEM) observations of solvent-etched foams and DSC measurements were used to reveal the possible origin of these microstructures, as well as the effects of die temperature and the introduction of nanoclay on them.

Experimental Section

Materials. A linear HPP, 3762, with a melt flow rate of 18 g/10 min was provided by Total Petrochemicals. Maleic anhydride grafted polypropylene (PP-MAH, Polybond 3150) with a melt flow rate of 50 g/10 min and a maleic anhydride level of 0.5 wt % was supplied by Chemtura Corporation and used as a coupling agent (CA). Cloisite 20A, manufactured by Southern Clay Products Inc., is a natural montmorillonite modified with dimethyl dehydrogenated tallow quaternary ammonium chloride. CO_2 with a purity of 99.5% (Linde Gas) was used as a physical blowing agent.

Table 1. CA and Clay Contents and Thermal Properties of HPPCA Blends and HPPC Nanocomposites

sample	CA content (wt %)	sample	clay content (wt %)	CA content (wt %)	T_m (°C)	T_c (°C)
–	–	HPP	0	0	161.0	120.0
HPPCA-1	4.8	HPPC0.5	0.5	4.8	161.0	120.0
HPPCA-2	9.5	HPPC1.0	1.0	9.5	161.5	119.5
HPPCA-3	19.0	HPPC2.0	2.0	19.0	161.0	120.0
HPPCA-4	47.5	HPPC5.0	5.0	47.5	160.5	118.5

Nanocomposite Preparation. HPP, CA, and clay were vacuum-dried at 80 °C for 8 h before use. The HPP was dry blended using the same amount of CA, and an HPP/clay premix was prepared by dry blending HPP and CA mixtures with the clay. The premix was subsequently melt extruded using a counter-rotating twin-screw compounder by maintaining a temperature of 200 °C with a rotator speed of 150 rpm. The clay content prepared for the master batch was 5 wt %. A series of nanocomposites with clay contents of 0.5, 1, 2, and 5 wt % were obtained by diluting the master batch with HPP; they are denoted as HPPC0.5, HPPC1.0, HPPC2.0, and HPPC5.0, respectively. Considering the large amount of CA used in each composition, HPP/CA blends having the same CA contents as the corresponding HPPC samples were prepared in this study for comparison, as shown in Table 1.

Extrusion Foaming. The single extrusion foaming system used in this work was described previously.[4] A filamentary die with length $L = 0.413$ in. and diameter $D = 0.051$ in. was used for the foaming experiments. The CO_2 content injected into the barrel, which was fixed to 5 wt % throughout the experiments, was accurately adjusted and regulated by controlling both the gas flow rate of the syringe pump and the material flow rate that passed through the die. When the polymer/gas solution entered the filament die, it experienced a rapid pressure drop, which caused a sudden decrease in gas solubility in the polymer; hence, a large number of bubbles were nucleated in the polymer matrix, and a foam structure was finally produced, followed by bubble growth. The die temperature here was equivalent to the temperature of the die and the heat exchanger. The foamed samples at different die temperatures were collected for observation of the cell morphology and measurement of the density.

Characterization. To investigate clay dispersion and exfoliation, HPPC nanocomposite pellets were hot-pressed at 200 °C to make a film for XRD analysis. XRD scans were made using a Siemens D5000 diffractometer in reflection mode with an incident X-ray wavelength of 1.54 Å at a scan rate of 1.0°/min over the range of $2\theta = 1-10°$.

The melting peak (T_m) and crystallinity of HPP and HPPC samples before and after foaming were determined using a Q2000 apparatus (TA Instruments) calibrated with indium. For all of the samples, only the data obtained from the first heating were recorded to elaborate the possible effect of foaming history on the crystallization behavior of HPP. The heating rate of the DSC tests was fixed at 20 °C/min unless otherwise indicated. The degree of crystallinity was calculated from the integration of the DSC melting peaks, using 290 J/g as the heat of fusion (ΔH_m) of 100% crystallized PP.[48]

Dynamic rheological measurements were carried out on a strain-controlled ARES rheometer (TA Instruments), using a 25-mm parallel-plate geometry and a 1-mm sample gap. Dynamic shear measurements were performed at frequencies from 0.01 to 70 rad/s at a temperature of 190 °C using strain values determined by a stress sweep to lie within the linear viscoelastic regions.

The foams were chemically treated by 7% potassium permanganate/sulfuric acid solution, as reported by Almanza et al.,[49] to reveal the crystalline morphology. The morphologies of the foamed samples were observed with a JEOL JMS 6060 scanning electron microscope. The samples were freeze-fractured in liquid nitrogen and sputter-coated with platinum. Both cell size and density were determined from the SEM micrographs. The cell density (N_0), the number of cells per cubic centimeter of unfoamed polymer, was determined from the equation

$$N_0 = \left(\frac{nM^2}{A}\right)^{3/2}\phi \quad (1)$$

where n is the number of cells in the SEM micrograph; M is the magnification factor; A is the area of the micrograph (in cm^2); and ϕ is the volume expansion ratio of the polymer foam, which can be calculated in accordance with the equation

$$\phi = \frac{\rho}{\rho_f} \quad (2)$$

where ρ and ρ_f are the mass densities of the sample before and after foaming, respectively, which were measured by the water displacement method in accordance with ASTM D792.

Results and Discussion

Dispersion of Nanoclay in HPP. Because of the nonpolar characteristics of the molecular chain of PP, its interactions with nanoclay are relatively weak. Consequently, it is very difficult for a PP chain to intercalate into the clay gallery and form fine nanocomposites. A coupling agent, such as PP-MAH, is often added to achieve a favorable energy change by increasing the magnitude and number of favorable polymer−clay interactions originating from the strong hydrogen bonding between the MA group of PP-MAH and the polar clay surface.[18,50,51] In this case, the content of MA relative to clay is critically important in determining the intercalation or exfoliation process. For commercial PP-MAH, however, only a very low MA grafting degree is available, because too much MA introduction usually significantly reduces the viscosity of PP-MAH and a CA with a lower viscosity can weaken the clay dispersion in the PP matrix because of the lower stresses that can be imposed on the clay particles during the compounding process.

The nanoclay used in this study is a commercial clay product that is a natural montmorillonite modified with dimethyl dehydrogenated tallow quaternary ammonium chloride. A twin-screw extruder was used to disperse the nanoclay in the PP resins, and 47.5 wt % CA was used as the coupling agent. An HPP/clay nanocomposite master batch with a clay content of 5 wt % was produced first and then was diluted with pure PP to lower the clay content, to 0.5, 1.0, and 2.0 wt %.

Figure 1 shows the XRD spectra of HPPC nanocomposites. It can be seen that clay 20A has an apparent 001 peak at $2\theta = 3.5°$, which corresponds to the layer spacing of 2.5 nm. After melt compounding of the clay with HPP, the 001 peak of HPPC5.0 (master batch) disappeared; instead, a very broad peak, indicating a half-exfoliated clay structure, was formed in

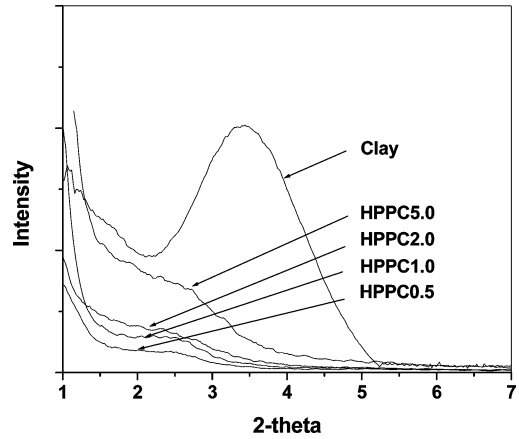

Figure 1. XRD spectra of clay and HPPC nanocomposites.

HPPC5.0. This result suggests that the presence of a coupling agent facilitated the insertion of PP chains into the clay galleries and destroyed the periodic layered structure of the clay. Upon further dilution of the master batch with pure PP, the intensity of the diffraction peak of PP/clay nanocomposites decreased gradually, demonstrating an increased degree of exfoliation in HPPC with a low clay content. It should be pointed out that, through the dilution process, the coupling agent content decreased dramatically to 19.0% in HPPC2.0, 9.5% in HPPC1.0, and 4.8% in HPPC0.5, as shown in Table 1. These results suggest that the diluting process that disperses nanoclay in the polymer matrix is highly efficient. Similar experimental results have been reported in our laboratory, where improved clay dispersion was realized in low-density polyethylene (LDPE)/clay,[28] metallocene polyethylene (mPE)/clay/wood fiber,[30] and PP/clay nanocomposites.[18] There are two possible reasons for this phenomenon: The first is that the clay−clay interaction decreases dramatically in the first processing, so that the polymer chains diffuse more easily into the clay interlayer in the dilution processing that follows. Moreover, the dilution processing extends the residence time of the polymer melt in the extruder, which obviously tends to affect the dispersion of the clay in the polymer matrix.[50−52] The second reason is that the CA tends to disperse around and into the nanoclay layer because of the strong interaction between MA in PP-MAH and clay[51] and a small amount of CA seems sufficient to saturate the PP−clay interface.

Cell Structure Evolution in HPP and HPPC Nanocomposite Foams. Figures 2 and 3 show the cell structures of HPP, HPP/CA-2, and HPPC nanocomposite foams at different die temperatures. As expected, poor foam morphologies, namely, large cell sizes, a small number of cells, and nonuniform cell distributions, were observed in HPP foams. This occurred because serious cell coalescence caused the cells to open and form interconnections with one another in the PP matrix.[16] With decreased die temperatures, only a slight improvement in foam morphology was observed. This result demonstrates that the decreased die temperature did not effectively improve the melt strength of PP and that serious cell coalescence was still present during HPP extrusion foaming. For comparison, extrusion foaming of HPP/CA was also carried out, and Figure 2 shows the cell morphologies of HPP/CA-2 foams obtained at various die temperatures. The introduction of CA did not obviously improve the cell morphology of HPP foams.

In HPPC nanocomposite foams, as seen in Figure 3, there was serious cell coalescence in HPPC0.5 and HPPC1.0 foams at a die temperature of 140 °C. Compared with the cell morphologies of pure HPP foams, however, those of HPPC0.5

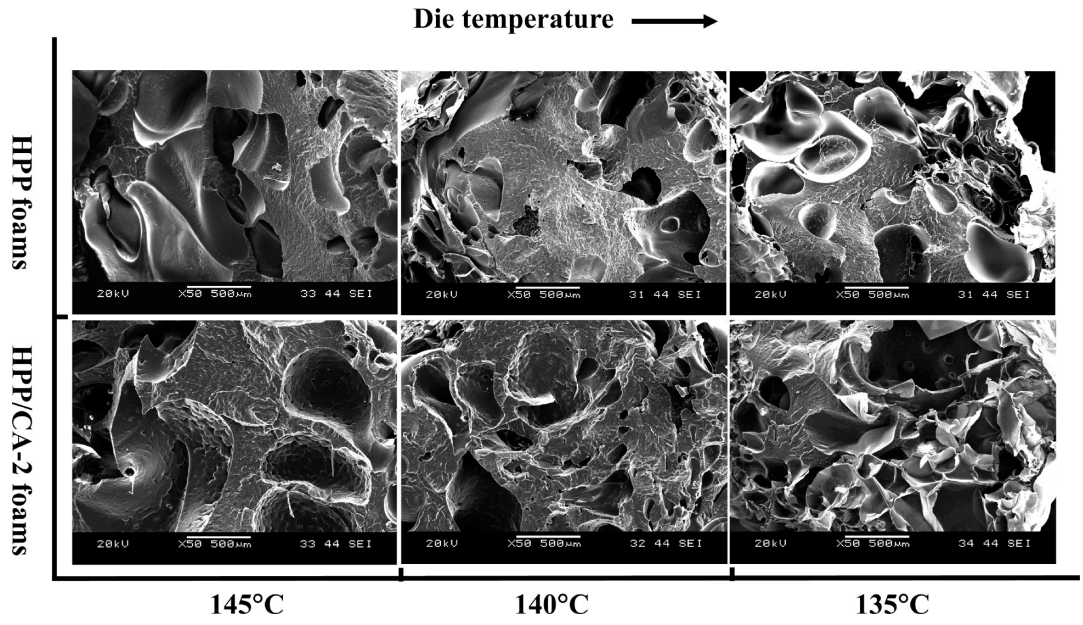

Figure 2. Cell structure evolution of HPP and HPP/CA-2 foams with die temperature.

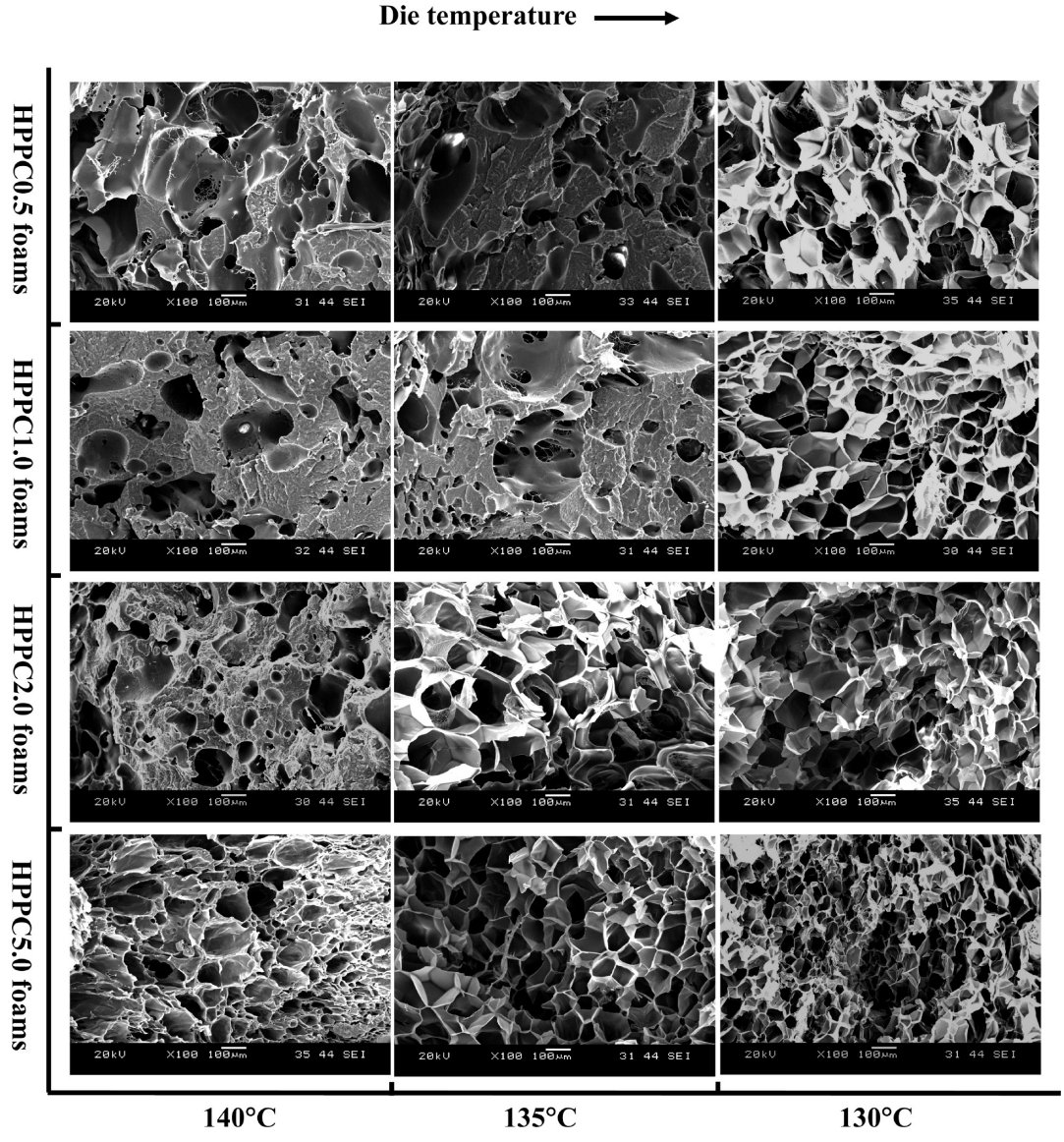

Figure 3. Cell structure evolution of HPPC nanocomposite foams with die temperature and clay content.

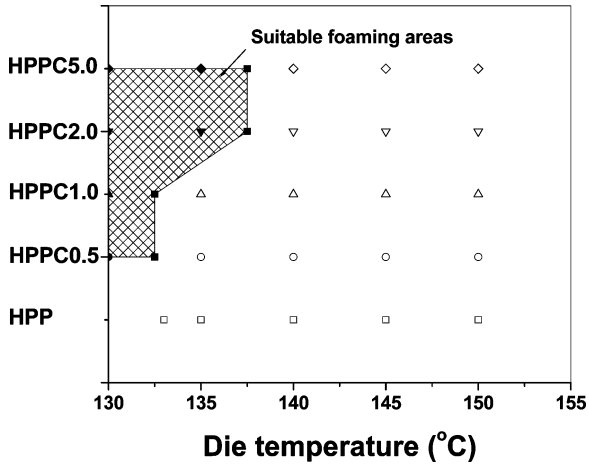

Figure 4. Suitable foaming window of HPP and HPPC nanocomposites in fabricating foams with well-defined cell morphology.

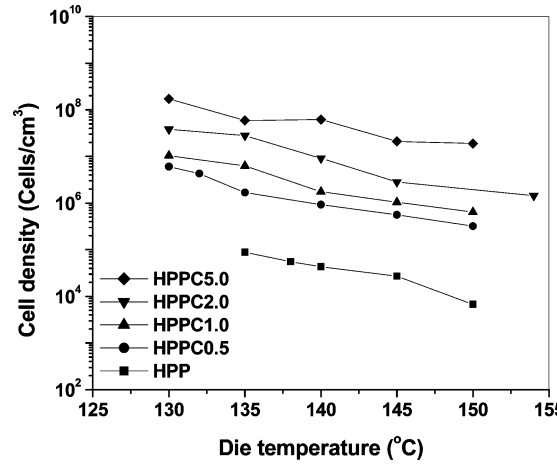

Figure 5. Cell densities of HPP and HPPC nanocomposite foams prepared at different die temperatures.

and HPPC1.0 foams were still clearly improved, indicating the positive effect on cell morphology of introducing nanoclay. With an increased clay content, the cell morphologies of HPPC foams improved continuously: smaller cell sizes, higher cell densities, higher close cell contents, and more uniform cell distributions were observed in HPPC2.0 and HPPC5.0 foams. These results clear showed that increased clay contents tended to improve the cell morphology of HPP foams up to 5.0%. When the die temperature was decreased to 135 °C, the cell morphologies of HPPC0.5 and HPPC1.0 foams did not change relative to those at 140 °C. At higher clay contents of 2.0 and 5.0 wt %, however, HPPC foams exhibited a dramatic improvement in cell structure, such as the presence of very thin cell walls and uniform cell size dispersions. It is well-known that a decreased melt temperature tends to increase the melt strength of a polymer to some extent. This increase in melt strength did not have an obvious effect on the cell morphology of HPP foams, but presented dramatically in HPPC2.0 and HPPC5.0 foams. At a lower die temperature of 130 °C, all HPPC nanocomposite foams exhibited well-defined cell morphologies.

A foaming window is a critical parameter by which the foamability of polymer resin can be evaluated. In general, a broad foaming window facilitates foam processing, whereas a narrow foaming window tends to make higher demands on the foaming system and particularly on the temperature control system. A polymer's foamability has been found to be relative to the structure of polymer.[3] Unlike amorphous polymers, crystalline polymers have a viscosity that is weakly temperature dependent before crystallization occurs, resulting in a narrower foam processing temperature range. Figure 4 shows a suitable foaming window for HPP and HPPC nanocomposites with respect to the die temperature, which was decreased from 150 to 130 °C. The suitable foaming window in this figure means that the foams obtained in those foaming regions had well-defined cell structures with very thin walls and uniform cell distributions. In the pure HPP, no suitable foaming window was found in this study because of serious cell coalescence. With the introduction of 0.5 wt % nanoclay, however, HPPC0.5 could produce good foamed samples at a die temperature of about 132.5−130 °C. This result indicates that the suitable foaming window for HPPC0.5 in this study was only 2.5 °C. At higher clay contents of 2.0 and 5.0 wt %, a broader foaming window of about 7.5 °C could be obtained in preparing good foamed samples. Therefore, the introduction of nanoclay improved the foaming window of HPP.

Mechanisms of Improvement in Cell Morphology with Nanoclay. Cell density is a parameter by which to show the number of surviving cells (per unfoamed unit volume) that have undergone the processes of cell nucleation, collapse, and coalescence. It has been used by many researchers to investigate the cell nucleation process. Figure 5 shows the cell densities of HPP and HPPC nanocomposite foams at different die temperatures. It can be seen that the cell density of HPP foams is quite low, namely, 10^3-10^5 cells/cm^3, and the decreased die temperature slightly increases their cell density. With the introduction of 0.5 wt % nanoclay, however, the cell density of HPPC0.5 foams dramatically increases to 10^5-10^7 cells/cm^3, possibly as a result of enhanced cell nucleation. With further increases in the nanoclay content, the cell densities of HPPC1.0 and HPPC2.0 foams increase gradually to 10^6-10^7 cells/cm^3. For these HPPC nanocomposite foams, a similar temperature dependence of cell density on the die temperature was observed. At a higher clay content of 5 wt %, HPPC5.0 foams exhibited a higher cell density of about 10^7-10^8 cells/cm^3 and presented a slight dependency on the die temperature.

The improved cell morphology that occurs with the introduction of nanoparticles has been found in various polymer/filler nanocomposites foaming systems that use a continuous method,[18,19,28−31,34,36] and mechanisms behind this phenomenon have been proposed.[53] In general, the presence of nanoparticles in a polymer melt tends to decrease the energy barrier to cell nucleation. A recent study by Wang et al.[27] confirmed that the presence of particles tends to induce a local stress variation in polymer/gas solutions that tends to reduce the critical bubble radius significantly.[53] In the case of HPPC nanocomposite extrusion foaming, because of the presence of high stress variations around the well-dispersed nanoclays, the critical bubble size decreases dramatically. Therefore, cell nucleation will be promoted, and the number of nucleated bubbles will be determined by the amount of efficient nucleating agent. The dispersion of nanoclays in HPP matrix is shown in Figure 1. It was found that nanoclay exhibited a half-exfoliated structure in the HPP matrix at low clay contents of 0.5, 1.0, and 2.0 wt % and that the degree of nanoclay exfoliation tended to decrease at the higher clay content of 5.0 wt %. In this study, the higher nanoclay content seemed to induce higher cell nucleation based on the cell density of HPPC foams.

The cell growth process is an extensional flow of the polymer/gas solution in nature.[41] The factors that affect the viscoelastic properties of a polymer melt usually affect its foaming behavior. Figure 6 shows the complex viscosities of HPPCA and HPPC

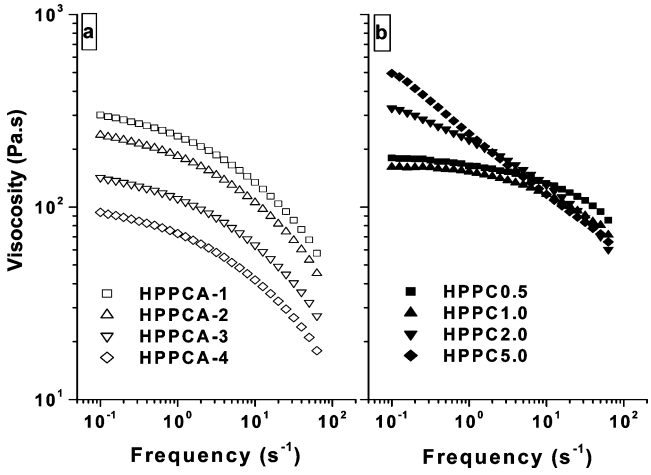

Figure 6. Complex viscosity curves of (a) HPPCA and (b) HPPC nanocomposites. The test temperature was 190 °C.

nanocomposites at a test temperature of 190 °C. For HPP/CA, no Newtonian plateau was observed at any of the measured frequency scopes, and the presence of a large amount of CA with high melt flow index (MFI) obviously decreased the melt viscosity of HPP. At a frequency of 0.1 s^{-1}, for example, the melt viscosity of HPP/CA decreased from 300.9 Pa·s for HPPCA-1 to 237.1 Pa·s for HPPCA-2, 142.2 Pa·s for HPPCA-3, and 93.8 Pa·s for HPPCA-4. With the introduction of a small amount of nanoclay, however, the complex viscosity of HPPC0.5 and HPPC1.0 melts exhibited a weak frequency dependency at a low frequency. Meanwhile, their melt viscosities were somewhat lower than those of the corresponding HPPCA-1 and HPPCA-2 materials. The introduction of nanoclay generally tends to increase the viscosity of composites, and the introduction of low clay loadings at below the percolation threshold, for example, normally results in a small increase in viscosity.[54] In this study, increased clay content was associated with an increase in CA content, which could weaken the effect of nanoclay loading on the viscosity of composites. Upon increasing the nanoclay content, however, a dramatic increase in melt viscosity was observed in HPPC2.0 and HPPC5.0 at low frequencies, whereas their counterparts, HPPCA-3 and HPPCA-4, exhibited an obvious decrease in viscosity due to the addition of a large amount of low-viscosity CA. This phenomenon suggests that the addition of high content s of clay significantly affected the viscosity and masked the negative effect of the CA on the viscosity of the composites. On the other hand, the presence of shear thinning and the absence of a Newtonian plateau were also recorded in HPPC2.0 and HPPC5.0. These results indicate that the introduction of well-dispersed nanoclay could dramatically affect the viscoelastic properties of the HPP melt.

The presence of shear thinning in the dynamic test and strain hardening in the extension test have been related to the orientation of nanoclay in polymer melt flow.[19,39,40] During foam processing, nanoclays tend to orient in the polymer flow direction because of the imposed shear force of the screw and extensional force of the channel die.[35] Once the polymer/gas mixture experiences a pressure drop in the die, cell nucleation occurs, induced by gas supersaturation, and is followed by cell growth. Cell growth tends to apply an extensional force on the cell wall and induces the orientation of the nanoclay around the cell wall, as observed by transmission electron microscopy (TEM).[16] In this situation, the nanoclay works like a second layer, stabilizing the cell structure and suppressing cell coalescence.[16] This means that a large amount of nucleated bubbles can survive during foaming processing.

High-magnification SEM was used to further investigate the effect of added nanoclay on the cell growth process during HPP foaming. Figure 7 shows the cell wall structures of HPPC2.0 at 135 °C and HPPC5.0 at 140 °C. It can be observed from the low magnification images that the foamed HPPC samples exhibited cell coalescence due to slightly higher die temperatures. At high magnification, it is interesting to note a large number of tiny cells of about 0.2−2 μm in size located in the

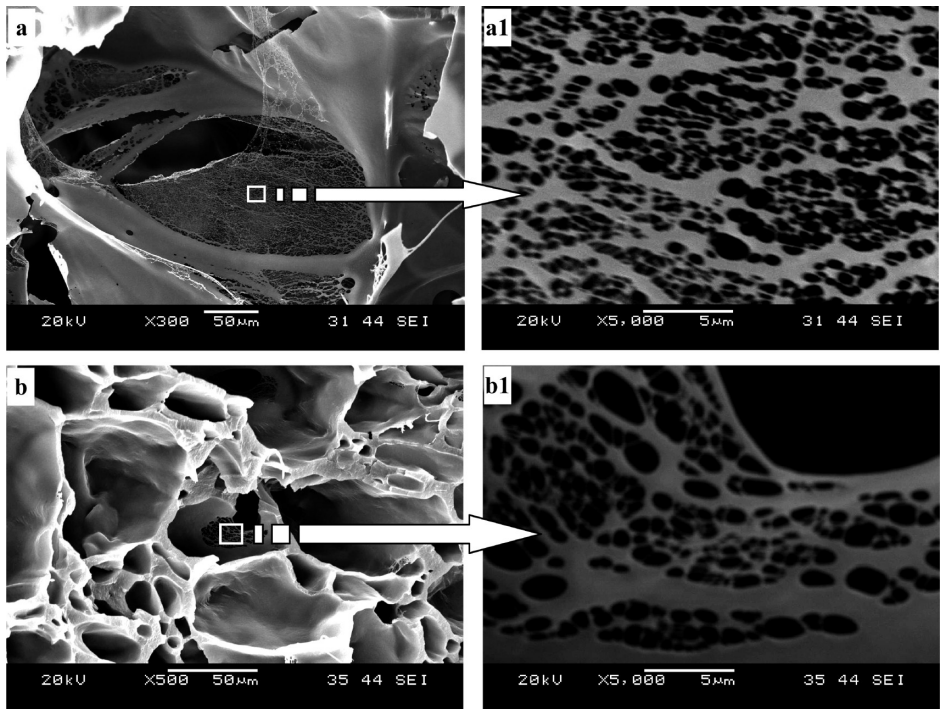

Figure 7. Cell wall structures of (a,a1) HPPC2.0 and (b,b1) HPPC5.0 nanocomposite foams. The foams were obtained at low die temperatures of 135 and 140 °C, respectively, and the CO_2 content was 5%.

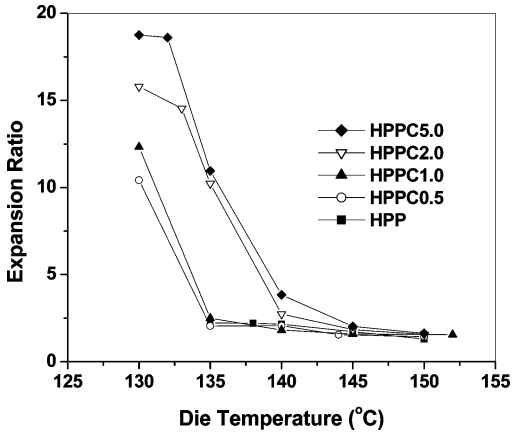

Figure 8. Expansion ratios of HPP and HPPC nanocomposite foams prepared at different die temperatures.

cell walls that seemed to create a network of very small cavities separated by microfibrils. In some areas where microfibrils had ruptured, larger cavities with nonuniform dimensions appeared. It should be noted that these kinds of tiny cells were absent in pure HPP foams. Therefore, it is believed that the tiny cells were mainly induced by the presence of well-dispersed nanoclay. A similar phenomenon has been reported in poly(lactic acid) (PLA) extrusion foaming,[55] where the tiny cells were present in PLA foams with a high expansion ratio. The authors attributed this phenomenon to crystal development in the cell wall as a result of a stretching-induced crystallization that stabilized the cell structure. Similarly, in this study, the presence of well-dispersed nanoclays dramatically increased the melt viscosity and melt strength of PP/clay nanocomposites, which lessened the occurrence of cell coalescence.

The expansion ratio is an important parameter describing the amount of gas that is retained and used during foam expansion, and the expansion ratio usually includes the contributions of cell nucleation, opening, and growth. Figure 8 shows the expansion ratios of HPP and HPPC nanocomposite foams at various die temperatures. HPP foams exhibited a very low expansion ratio of about 1.7−2.2, and a decrease in die temperature did not have any obvious effect on foam expansion. With the introduction of 0.5 wt % nanoclay, however, the expansion ratio of HPPC0.5 significantly increased to 10.0 at the die temperature of 130 °C, even though the same amount of gas was injected during HPP and HPPC0.5 foam processing. This result demonstrates that more gas was retained for foaming with the introduction of nanoclay, as a result of the reduced degree of cell opening through the increased melt strength, as well as the increased tortuosity of the gas diffusion channel around the aligned nanoclay particles. With an increased clay content, the highest expansion ratio increased gradually to 12.3 at HPPC1.0, 15.8 at HPPC2.0, and 18.8 at HPPC5.0. Furthermore, the high clay content facilitated foam expansion at even high die temperatures.

The well-dispersed nanoclay enhanced cell nucleation by decreasing the critical bubble radius through the presence of high local stress variations around the clay particles[27] and suppressed cell coalescence by increasing the melt strength. This means that more cells could form in the cell nucleation stage and that most of them could survive and then steadily grow in the cell growth stage. Furthermore, the oriented nanoclays might occur during cell growth that increased the tortuousity of gas diffusion path. All of these effects were beneficial to an increase of cell density and foam expansion in HPP foams with the introduction of well-dispersed nanoclays.

Formation of Crystal-Induced Microstructures in Cell Walls. Figure 9 shows the cell wall structures of foamed HPP and HPPC nanocomposites. At a die temperature of 150 °C, HPP foam had a large number of polygon-shaped microstructures in the cell walls, and the cell walls were thick. These microstructures had various sizes in the range of 30−60 μm, and they touched each other. In some locations, small holes with a size of 5−8 μm were observed among the microstructures. The number of cells with microstructures had a direct relationship to the die temperature. At a low die temperature of 133 °C, for example, the microstructures in HPP foam were present in only a very few cells located at the foam's core. For cells near the foam's skin, however, the microstructures were absent in the cell walls, which were thin. This phenomenon suggests that the microstructures in cell walls tend to change with the die temperature, as well as the thickness of the cell walls. Similarly, the microstructures were also observed in HPPC5.0 foam obtained at 150 °C. Compared to HPP foam, however, HPPC5.0 foam had microstructures that decreased significantly to 5−25 μm. At a low die temperature of 135 °C, the foamed HPPC5.0 sample was highly expanded, the cell walls were very thin at about 1−2 μm, and the cell wall surfaces were very smooth, indicating an absence of microstructure in the cell walls. It is clear from the SEM observations shown in Figure 9 that the presence or absence of microstructures had no direct relationship on whether nanoclay was introduced, but rather depended on the cell wall thickness. In the case of a thick cell wall, microstructures tended to form within the cell wall, and the added nanoclay reduced the size of the microstructures. With a thin cell wall, the microstructure tended to be absent.

The microstructures shown in Figure 9 seem to be crystal structures. The evolution of these microstructures with the introduction of nanoclay is similar to the effect of nanoclay on crystal size.[56] SEM was used to assess the morphology of the crystalline phase. For this purpose, the foams were chemically treated to reveal the crystalline morphology by removing the amorphous phase.[49] Figure 10 shows micrographs of the foams after they had been chemically etched. Figure 10a shows that some original microstructures were unclear and some of them were replaced by embedded spherical particles. Examination of the high-magnification SEM micrograph clearly shows that the spherical particles are spherulites, with a lamellar structure on their surface. In the case of thin cell walls, as illustrated in Figure 10b, the chemical treatment did not obviously change the cell wall structure at low magnification. At high magnification, however, a large number of very small crystals were observed in the cell wall. It seems that a higher degree of biaxial stretching on the cell walls during cell growth induced smaller-sized spherulite crystals. This result suggests that the roughness of cell walls was associated with the size of crystal domains, where the large-sized crystals led to the formation of microstructures and small-sized crystals caused the absence of microstructures in the cell walls.

Distribution of Crystal Sizes across the Foamed Sample. Although the crystallization behaviors of PP under high gas pressure are well understood,[46,57] the crystallization of PP during continuous extrusion foaming has not been studied extensively. In this study, it was possible to qualitatively speculate on the crystal size distribution in the foamed sample based on the smooth level of cell walls. As Figure 9b shows, the presence of microstructures in the foam's core was associated with the formation of large-sized crystals, whereas the cell walls were smooth near the foam's skin, and small-sized crystals tended

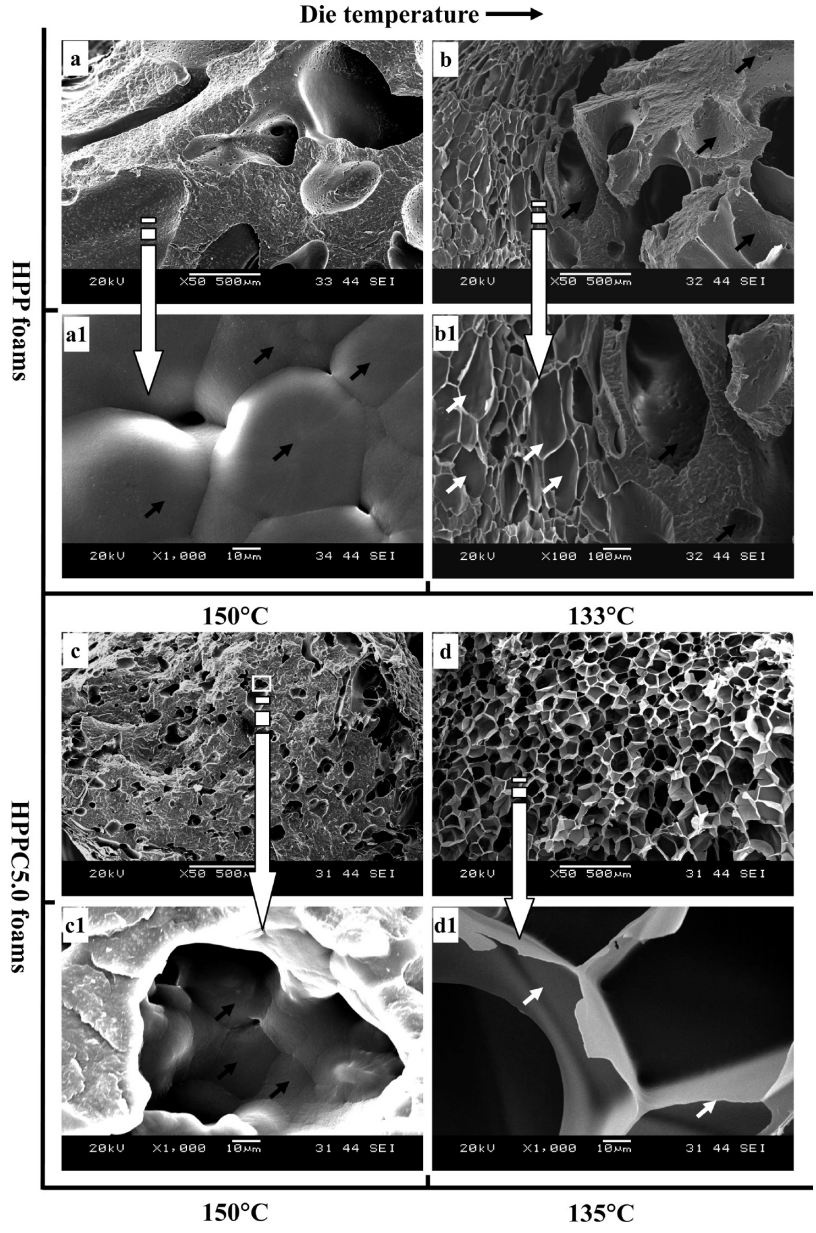

Figure 9. Presence and absence of microstructure in cell walls of HPP and HPPC5.0 foams obtained at various die temperatures.

to form there. Thus, the crystal size exhibited a broad distribution across the foamed sample.

During the extrusion foaming of crystalline polymer, the crystallization behavior of polymeric foams can be affected in two ways. One is the potential for polymer to crystallize inside the extruder die before foam expansion. During extrusion processing, researchers have found that the temperature of a polymer melt cannot be completely uniform in the extruder and the polymer flow rate near the die is extremely low. As in PP extrusion foaming, once the die temperature of 150−130 °C is lower than the melting peak of gas plasticized PP, the polymer melt near the die at this juncture can crystallize isothermally, and the formed crystals can affect the crystallization behavior of the foamed sample. Because of a lack of experimental data, we cannot quantitatively explain the possible effect of this phenomenon on the crystallization behavior of PP during the foam processing stage.

The second thing that can affect the crystallization behavior of polymeric foams is polymer crystallization outside of the extruder die during foam expansion. It is known that foam expansion is accompanied by a gas cooling process with a very high cooling rate,[58] which is described as the local cooling effect of expanded gas. Local cooling can affect each cell wall's crystallization behavior. For a gas expanding foaming sample, the gas cooling effect will lead to a temperature gradient across the foamed filament, especially in low-density foam processing, where the core has a high temperature and the skin has a lower one. The temperature gradient usually affects crystal growth, with the larger-sized crystal in the foam core corresponding to the longer time provided for its growth and a smaller-sized crystal near the foam skin corresponding to a shorter growth time. In polymeric foaming, the temperature gradient can induce another effect. It is known that cell walls are strongly extended during cell growth and that the effect of this stretching on crystal size can be explained by the expansion ratio, that is, the degree of stretching at the cell walls. As shown in Figures 7 and 8, it was found that a higher degree of stretching led to a smaller crystal size in the cell walls.[59,60] The rapidly cooled skin increases the polymer melt's strength, and the higher degree of stretching can be applied to the cell wall during cell growth,

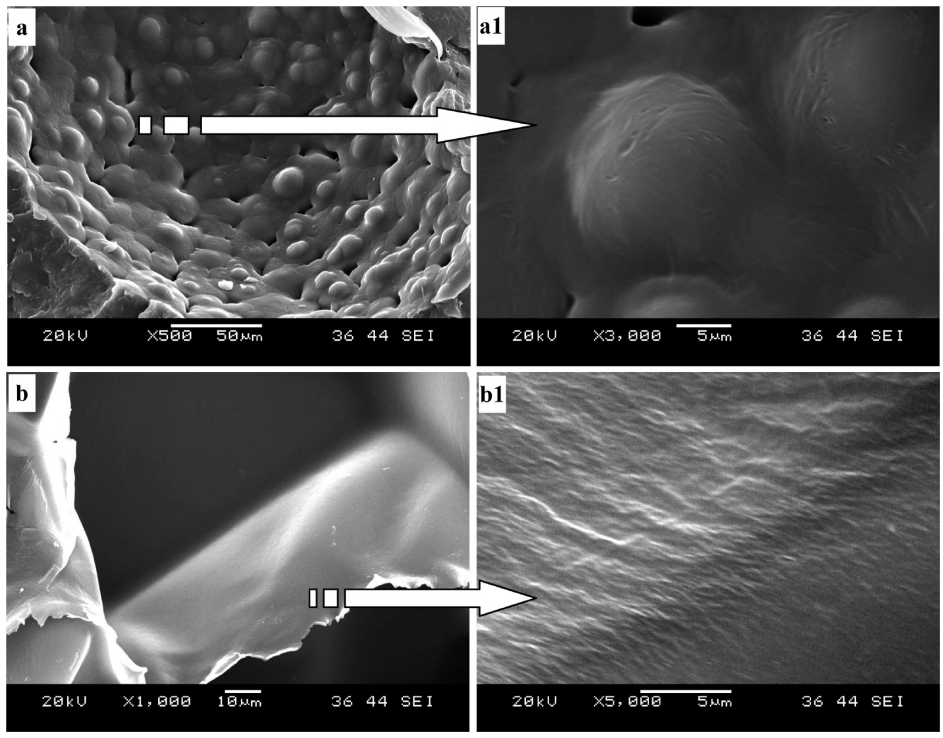

Figure 10. Micrographs obtained after etching of cell walls. (a,a1) HPP foam obtained at a die temperature of 140 °C and (b,b1) HPPC5.0 foam obtained at a die temperature of 135 °C.

which leads to the formation of more smaller-sized crystals compared with the core, where the cell walls have a greater tendency to coalesce and their stretching might not have much affect on crystallization.

In addition to the possible effects of the temperature gradient, the presence of a large amount of gas can plasticize the polymer matrix, decrease the crystallization temperature,[46] change the crystallization time, and thus affect the crystallization behavior of the foamed sample and the crystal morphology of the formed crystals during cell growth. As reported by Almanza et al.,[47] the crystalline clusters formed "spherical cap-shaped crystals" in the cell walls of LDPE foams, which is very different from the crystal morphology of the well-defined spherulites in the solid LDPE sheet. Similar observations were also verified by the crystal morphology of foamed PP in this study.

It was seen that the die temperature affected the crystal size in the cell walls. At a higher die temperature, most of the cells with large-sized crystals were observed in the foamed samples because of their longer crystallization time, whereas at a lower die temperature, only a few cells in the foam's core had large-sized crystals.

The introduction of nanoclay dramatically affected the crystal size in the cell walls. At a higher die temperature, large-sized crystals were observed in the cell walls. However, compared with the HPP foam crystals obtained at the same die temperature, as shown in Figure 9, the crystals in the HPPC foam were much smaller. This phenomenon can be attributed to enhanced crystal nucleation due to the presence of nanoclay.[55] At a lower die temperature, we could observe only small-sized crystals, even at the foam's core. This can be explained by the increased melt strength caused by the addition of well-dispersed nanoclay to support the cells' steady growth, with the strong stretching force enhancing crystal nucleation and facilitating the increase in crystal density and the decrease in crystal size.[58,59]

DSC Curves of HPP and HPPC before and after Continuous Extrusion. DSC curves were used to further study the effect of extrusion foaming on the crystallization behaviors of HPP and HPPC. Figure 11 shows the melting behaviors of HPP and HPPC0.5 samples before foaming. It can be seen that only a single peak is present in the DSC curve of the HPP and HPPC samples. The melting peak temperature and crystallinity of pure HPP are about 164.2 °C and 40.6%, respectively. The introduction of nanoclay did not obviously affect the melting peak temperature and crystallinity of HPP (see Table 2), which indicates that the clay particles were not fully exfoliated to affect the molecular movement for crystal formation.

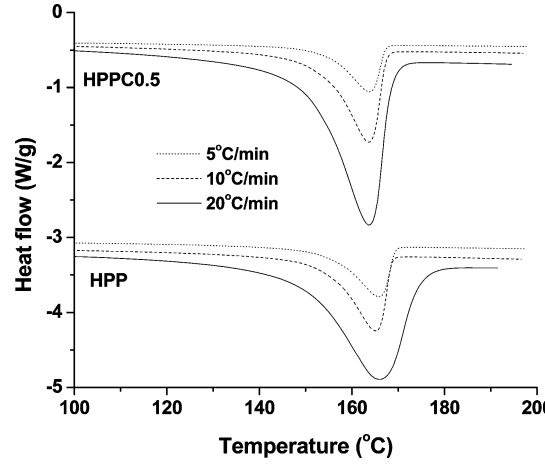

Figure 11. DSC curves of unfoamed HPP and HPPC0.5 samples measured at heating rates of 5, 10, and 20 °C/min, as indicated.

However, it seems that the extrusion foam process tended to slightly increase the crystallinity of the HPP and HPPC foams, as indicated in Table 2, where the crystallinities of the HPP and HPPC foams increased from 39−43% to 45−51%. On the other hand, the extrusion foaming process seems to have induced another melting peak in the DSC curves of HPP and HPPC. Figure 12 shows the melting behaviors of HPP and HPPC0.5 foams obtained at various die temperatures, and the small plots in Figure 12 show a detailed view of the DSC curves. For each

Table 2. Crystallinities of HPP and HPPC0.5 Samples before and after Extrusion Foaming

heating rate (°C/min)	HPP	HPP foams obtained at different die temperatures				
		150 °C	145 °C	140 °C	135 °C	133 °C
5	40.0	47.1	46.9	47.4	47.8	48.8
10	41.0	47.3	44.6	48.6	50.2	46.8
20	40.6	49.0	50.7	50.3	49.0	48.9

heating rate (°C/min)	HPPC0.5	HPPC0.5 foams obtained at different die temperatures				
		150 °C	145 °C	140 °C	135 °C	130 °C
5	39.4	47.0	46.8	48.1	50.0	48.5
10	39.6	45.8	49.0	48.1	50.2	47.5
20	42.8	46.4	48.9	50.8	48.2	50.0

sample, three different heating rates of 5, 10, and 20 °C/min were applied. For the HPP foams obtained at a die temperature of 150 °C, it was observed that a weak low melting peak (T_{m1}) was present in the DSC curve. Furthermore, the changed heating rate did not affect this peak's existence. At a lower die temperature, T_{m1} could still be observed in DSC curves; however, a decrease in die temperature tended to weaken ΔH_{m1}. The effect of the nanoclay particles on T_{m1} formation was investigated as well. Similarly, T_{m1} was also noticed in the DSC curves of HPPC0.5 foams at the die temperatures of 150 and 145 °C. Compared with the HPP foams obtained at the same temperatures, however, the HPPC0.5 foams had a T_{m1} with a lower intensity. As the die temperature decreased further to 135 and 130 °C, T_{m1} of HPPC0.5 foams disappeared, and the heating rate change did not lead to its presence in the DSC curves.

During the DSC test, only a first heating was applied to the samples. The processing thermal history can be extracted from the unfoamed samples, and both the processing thermal history and foaming history can be extracted from the foamed samples. Therefore, the T_{m1} peak, uniquely observed for the foamed samples, must have stemmed from the foaming action.

The presence of a shoulder peak in the DSC curve has been attributed to secondary crystallization that is a local phenomenon involving a section of a given chain and crystallization regions that are limited in the direct vicinity of primary lamellar crystals.[61] Secondary crystallization occurs after primary crystallization, and the formed crystals exhibit lower perfection compared with those formed during primary crystallization. During extrusion foaming of PP, cell nucleation occurs as a result of gas depressurization once the PP/gas solution nears the die. Afterward, the foamed sample gradually exits the die as bubble growth occurs, and the foaming sample's temperature decreases dramatically as a result of the cooling effect of the expanding gas and air circulation. At a high die temperature,

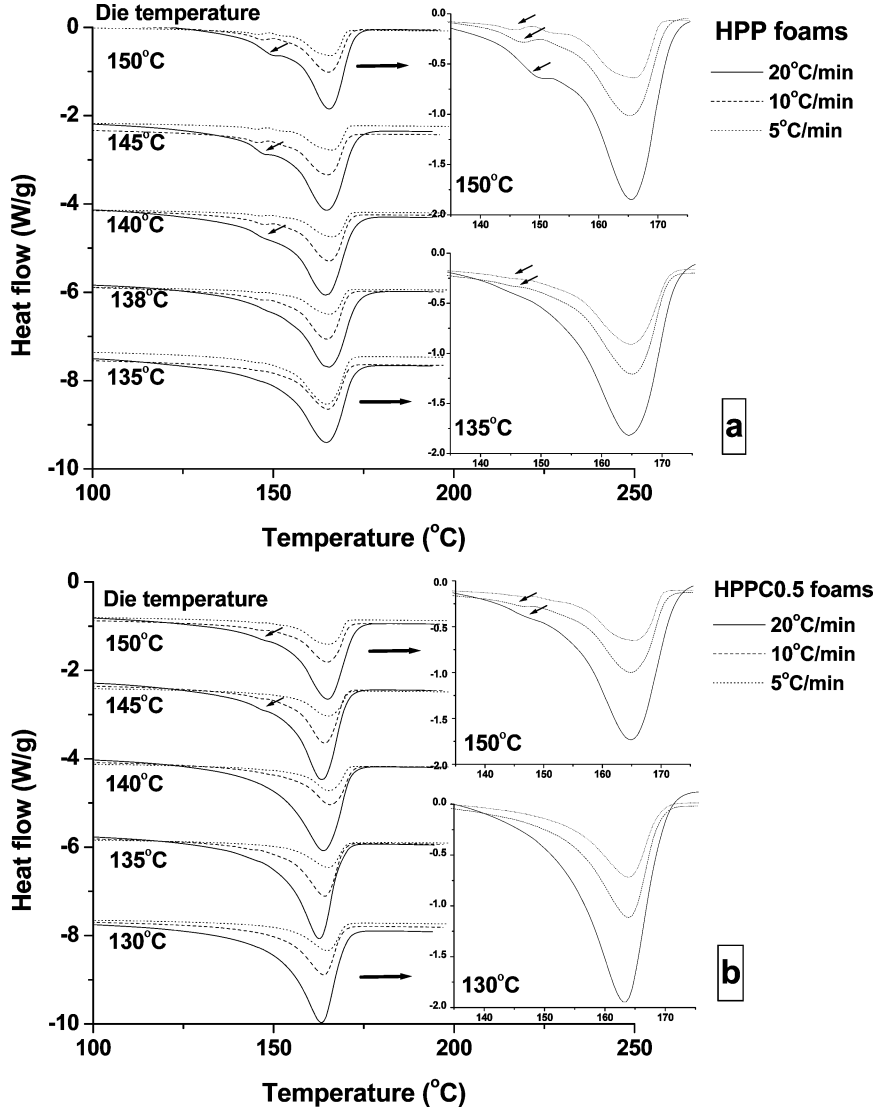

Figure 12. DSC curves of foamed (a) HPP and (b) HPPC0.5 samples. DSC tests were carried out at heating rates of 5, 10, and 20 °C/min, as indicated.

the crystals formed during the secondary crystallization process normally had a longer crystallization time in which to grow, resulting in a higher ΔH_{m1}. At a low die temperature, however, a shorter crystallization time for secondary crystals tended to reduce the value of ΔH_{m1}. The introduction of nanoclay seems to suppress the formation of secondary crystals, which might be due to enhanced crystal nucleation.

As shown in Figures 8 and 11, it is interesting to note that both the crystal size in the cell walls and T_{m1} showed similar relationships to the die temperature, where the presence of a great number of large-sized crystals corresponded to the formation of T_{m1} with high ΔH_m and a decrease in the number of large-sized crystals or a dramatic reduction of crystal size corresponded to a decrease of ΔH_m or the absence of T_{m1}. However, we cannot verify these relationships.

It should be pointed out that the crystallization process during crystalline polymer foaming is complex because of the potential for crystallization to occur inside the die before foam expansion, as well as the net effect of temperature and viscosity and the gas plasticization effect on the crystallization outside the die during foam expansion. Our present data are too limited for us to fully understand what crystallization takes place during PP foaming and why the cell wall thickness exhibits a direct relationship to the size of the crystals formed within it. Simulations of temperature and melt viscosity distributions in and out of the die during PP extrusion foaming will be made in the future to quantitatively analyze the process of PP crystallization behavior during foaming.

Conclusions

In this study, HPP and HPPC nanocomposite foams were fabricated by extrusion foaming, and the cell structure evolution of HPP foams with clay content and die temperature was investigated. An HPP/clay nanocomposite master batch with a half-exfoliated structure was successfully prepared by introducing 47.5 wt % PP-MAH as a coupling agent, and further dilution with pure PP increased the exfoliation degree of nanoclay in the HPP matrix. As expected, HPP exhibited poor foamability because of its weak melt strength. With the introduction of small amounts of nanoclay, however, an obvious increase in melt viscosity was observed. This tended to stabilize cell structure and thus significantly increased cell density and the expansion ratio of HPPC foams, in addition to enhancing cell nucleation as a result of the presence of large numbers of heterogeneous nucleating sites. A further increase in nanoclay content to 5 wt % led to an obvious increase in the suitable foaming window. Microstructures were found in the cell walls of the foamed HPP and HPPC nanocomposite foams, and they tended to evolve with the thickness of the cell wall depending on the die temperature. SEM observation revealed that microstructures formed by covering large-sized crystals and the absence of microstructures was due to a small crystal size in the cell wall. According to the SEM micrographs, a crystal size distribution was observed across the foamed samples, where the large-sized crystals were located in the foam's core whereas small-sized crystals were found near the foam's skin. The possible reasons behind this phenomenon are that the temperature gradient affected the crystallization time and that various degrees of cell wall stretching in different areas affected crystal size. The introduction of nanoclay enhanced crystal nucleation during HPP foaming, which dramatically decreased crystal size compared to that without nanoclay added at the same die temperature. DSC tests with different scanning rates indicated that the presence of T_{m1} in the foamed HPP and HPPC foams was related to the formation of secondary crystals and that ΔH_{m1} tended to decrease with decreasing die temperature. The addition of nanoclay seems to suppress the formation of secondary crystals, probably because its presence enhances crystal nucleation.

Acknowledgment

The authors are grateful to the Consortium of Cellular and Micro-Cellular Plastics (CCMCP) and to the Natural Sciences and Engineering Research Council of Canada (NSERC) for financial support of this project.

Literature Cited

(1) Vasile, C. Seymour, R. B. *Handbook of Polyolefins*; Marcel Dekker: New York, 1993.

(2) Colton, J. S. The Nucleation of Microcellular Foams in Semi Crystalline Thermoplastics. *Mater. Manuf. Processes* **1989**, *4*, 253.

(3) Burt, J. G. The Elements of Expansion of Thermoplastics Part II. *J. Cell. Plast.* **1978**, *14*, 341.

(4) Park, C. B.; Cheung, L. K. A Study of Cell Nucleation in the Extrusion of Polypropylene Foams. *Polym. Eng. Sci.* **1997**, *37*, 1.

(5) Zhai, W. T.; Wang, H. Y.; Yu, J.; Dong, J. Y.; He, J. S. Cell Coalescence Suppressed by Crosslinking Structure in Polypropylene Microcellular Foaming. *Polym. Eng. Sci.* **2008**, *48*, 1312.

(6) Rodrıǵuez-Peŕez, M. A. Crosslinked Polyolefin Foams: Production, Structure, Properties, and Applications. *Adv. Polym. Sci.* **2005**, *184*, 97.

(7) Spitael, P.; Macosko, C. Strain Hardening in Polypropylenes and Its Role in Extrusion Foaming. *Polym. Eng. Sci.* **2004**, *44*, 2090.

(8) Naguib, H. E.; Park, C. B.; Panzer, U.; Reichelt, N. Strategies for Achieving Ultra Low-Density PP Foams. *Polym. Eng. Sci.* **2002**, *42*, 1481.

(9) Zhai, W. T.; Wang, H. Y.; Yu, J.; Dong, J. Y.; He, J. S. Foaming Behavior of Isotactic Polypropylene in Supercritical CO_2 Influenced by Phase Morphology via Chain Grafting. *Polymer* **2008**, *49*, 3146.

(10) Liu, C.; Wei, D.; Zheng, A.; Li, Y.; Xiao, H. Improving Foamability of Polypropylene by Grafting Modification. *J. Appl. Polym. Sci.* **2006**, *101*, 4114.

(11) Han, D. H.; Jang, J. H.; Kim, H. Y.; Kim, B. N.; Shin, B. Y. Manufacturing and Foaming of High Melt Viscosity of Polypropylene by Using Electron Beam Radiation Technology. *Polym. Eng. Sci.* **2006**, *46*, 431.

(12) Danaei, M.; Sheikh, N.; Taromi, F. A. Radiation Cross-linked Polyethylene Foam: Preparation and Properties. *J. Cell. Plast.* **2005**, *41*, 551.

(13) Ruinaard, H. Elongational Viscosity as a Tool to Predict the Foamability of Polyolefins. *J. Cell. Plast.* **2006**, *42*, 207.

(14) Doroudiani, S.; Park, C. B.; Kortschot, M. T. Processing and Characterization of Microcellular Foamed High Density Polyethylene/Isotactic Polypropylene Blends. *Polym. Eng. Sci.* **1998**, *38*, 1205.

(15) Zhai, W. T.; Wang, H. Y.; Yu, J.; Dong, J. Y.; He, J. S. Foaming Behavior of Polypropylene/Polystyrene Blends Enhanced by Improved Interfacial Compatibility. *J. Polym. Sci. B: Polym. Phys.* **2008**, *46*, 1641.

(16) Okamoto, M.; Nam, P. H.; Maiti, P.; Kotaka, T.; Nakayama, T.; Takada, M.; Ohsima, M.; Usuki, A.; Hasegawa, N.; Okamoto, H. Biaxial Flow-Induced Alignment of Silicate Layers in Polypropylene/Clay Nanocomposite Foam. *Nano Lett.* **2001**, *1*, 503.

(17) Nam, P. H.; Maiti, P.; Okamoto, M.; Kotaka, T.; Nakayama, T.; Takada, M.; Ohshima, M.; Usuki, A.; Hasegawa, N.; Okamoto, H. Foam Processing and Cellular Structure of Polypropylene/Clay Nanocomposites. *Polym. Eng. Sci.* **2002**, *42*, 1907.

(18) Zheng, W. G.; Lee, Y. H.; Park, C. B. Use of Nanoparticles for Improving the Foaming Behaviors of Linear PP. *J. Appl. Polym. Sci.* **2010**, *117*, 2972.

(19) Werner, P.; Verdejo, R.; Wöllecke, F.; Altstädt, V.; Sandler, J. K. W.; Shaffer, M. S. P. Carbon Nanofibers Allow Foaming of Semicrystalline Poly(ether ether ketone). *Adv. Mater.* **2005**, *17*, 2864.

(20) Naguib, H. E.; Park, C. B.; Lee, P. C.; Xu, D. L. A Study on the Foaming Behaviors of PP Resins with Talc as Nucleating Agent. *J. Polym. Eng.* **2006**, *26*, 565.

(21) Lee, M.; Tzoganakis, C.; Park, C. B. Extrusion of PE/PS Blends with Supercritical Carbon Sioxide. *Polym. Eng. Sci.* **1998**, *38*, 1112.

(22) Lee, P. C.; Wang, J.; Park, C. B. Extruded Open-Cell Foams Using Two Semicrystalline Polymers with Different Crystallization Temperatures. *Ind. Eng. Chem. Res.* **2006**, *45*, 175.

(23) Rachtanapun, P.; Selke, S. E. M.; Matuana, L. M. Microcellular Foam of Polymer Blends of HDPE/PP and Their Composites with Wood Fiber. *J. Appl. Polym. Sci.* **2003**, *88*, 2842.

(24) Rachtanapun, P.; Selke, S. E. M.; Matuana, L. M. Effect of the High-Density Polyethylene Melt Index on the Microcellular Foaming of High-Density Polyethylene/Polypropylene Blends. *J. Appl. Polym. Sci.* **2004**, *93*, 364.

(25) Reichelt, N.; Stadlbauer, M.; Folland, R.; Park, C. B.; Wang, J. PP-Blends with Tailored Foamability and Mechanical Properties. *Cell. Polym.* **2003**, *22*, 315.

(26) Zhai, W. T.; Leung, S. N.; Wang, L.; Kuboki, T.; Park, C. B. The Effect of Nanoparticles on the Foaming Behavior of Polyolefin-Based Nanocomposites: Fundamental Issues. *Curr. Opin. Solid State Mater. Sci.*, manuscript submitted.

(27) Wang, C.; Leung, S. N.; Bussmann, M.; Zhai, W. T.; Park, C. B. Numerical Investigation of Nucleating Agent-Enhanced Heterogeneous Nucleation. *Ind. Eng. Chem. Res.*, manuscript submitted.

(28) Lee, Y. H.; Wang, K. H.; Park, C. B.; Sain, M. Effects of Clay Dispersion on the Foam Morphology of LDPE/Clay Nanocomposites. *J. Appl. Polym. Sci.* **2007**, *103*, 2129.

(29) Lee, Y. H.; Park, C. B.; Wang, K. H.; Lee, M. H. HDPE−Clay Nanocomposite Foams Blown with Supercritical CO_2. *J. Cell. Plast.* **2005**, *41*, 487.

(30) Guo, G.; Wang, K. H.; Park, C. B.; Kim, Y. S.; Li, G. Effects of Nanoparticles on Density Reduction and Cell Morphology of Extruded Metallocene Polyethylene/Wood Fiber Nanocomposites. *J. Appl. Polym. Sci.* **2007**, *104*, 1058.

(31) Han, X. M.; Zeng, C. C.; Lee, L. J.; Koelling, K. W.; Tomasko, D. L. Extrusion of Polystyrene Nanocomposite Foams with Supercritical CO_2. *Polym. Eng. Sci.* **2003**, *43*, 1261.

(32) Zeng, C. C.; Han, X. M.; Lee, L. J.; Koelling, K. W.; Tomasho, D. L. Polymer−Clay Nanocomposite Foams Prepared Using Carbon Dioxide. *Adv. Mater.* **2003**, *15*, 1743.

(33) Shen, J.; Zeng, C. C.; Lee, L. J. Synthesis of Polystyrene−Carbon Nanofibers Nanocomposite Foams. *Polymer* **2005**, *46*, 5218.

(34) Yuan, M. J.; Turng, L. S.; Gong, S. Q.; Caulfield, D.; Hunt, C.; Spindler, R. Study of Injection Molded Microcellular Polyamide-6 Nanocomposites. *Polym. Eng. Sci.* **2004**, *44*, 673.

(35) Yuan, M. J.; Song, Q.; Turng, L. S. Spatial Orientation of Nanoclay and Crystallite in Microcellular Injection Molded Polyamide-6 Nanocomposites. *Polym. Eng. Sci.* **2007**, *47*, 765.

(36) Zheng, W. G.; Lee, Y. H.; Park, C. B. The Effects of Exfoliated Nano-Clay on the Extrusion Microcellular Foaming of Amorphous and Crystalline Nylon. *J. Cell. Plast.* **2006**, *42*, 271.

(37) Zhai, W. T.; Yu, J.; Wu, L. C.; Ma, W. M.; He, J. S. Heterogeneous Nucleation Uniformizing Cell Size Distribution in Microcellular Nanocomposites Foams. *Polymer* **2006**, *47*, 7580.

(38) Okamoto, M.; Nam, P. H.; Maiti, P.; Kptaka, T.; Hasegawa, N.; Usuki, A. A House of Cards Structure in Polypropylene/Clay Nanocomposites Under Elongational Flow. *Nano Lett.* **2001**, *1*, 295.

(39) Park, J. U.; Kim, J. L.; Kim, D. H.; Ahn, K. H.; Lee, S. J. Rheological Behavior of Polymer/Layered Silicate Nanocomposites under Uniaxial Extensional Flow. *Macromol. Res.* **2006**, *14*, 318.

(40) Koo, C. M.; Kim, J. H.; Wang, K. H.; Chung, I. J. Melt-Extensional Properties and Orientation Behaviors of Polypropylene-Layered Silicate Nanocomposites. *J. Polym. Sci. B: Polym. Phys.* **2005**, *43*, 158.

(41) Stange, J.; Münstedt, H. Rheological Properties and Foaming Behavior of Polypropylenes with Different Molecular Structures. *J. Rheol.* **2006**, *50*, 907.

(42) Mandelkern, L. *Crystallization of Polymers*; McGraw-Hill: New York, 1964.

(43) Becjman, E.; Porter, R. S. Crystallization of Bisphenol a Polycarbonate Induced by Supercritical Carbon Dioxide. *J. Polym. Sci. B: Polym. Phys.* **1987**, *25*, 1511.

(44) Zhai, W. T.; Yu, J.; Ma, W. M.; He, J. S. Influence of Long-Chain Branching on the Crystallization and Melting Behavior of Polycarbonates in Supercritical CO_2. *Macromolecules* **2007**, *40*, 73.

(45) Ma, W. M.; Yu, J.; He, J. S. Direct Formation of Gamma Form Crystal of Syndiotactic Polystyrene from Amorphous State in Supercritical CO_2. *Macromolecules* **2004**, *37*, 6912.

(46) Naguib, H. E.; Park, C. B.; Song, S. W. Effect of Dupercritical Gas on Crystallization of Linear and Branched Polypropylene Resins with Foaming Additives. *Ind. Eng. Chem. Res.* **2005**, *44*, 6685.

(47) Almanza, O.; Rodríguez-Pérez, M. A.; Chrnev, B.; de Saja, J. A.; Zipper, P. Comparative Study on the Lamellar Structure of Polyethylene Foams. *Eur. Polym. J.* **2005**, *41*, 599.

(48) Wunderlich, B. *Macromolecular Physics, Vol. 1, Crystal Structure, Morphology, Defects*; Academic Press: NewYork, 1973.

(49) Almanza, O.; Rodríguez-Pérez, M. A.; De Saja, J. A. The Microstructure of Polyethylene Foams Produced by a Nitrogen Solution Process. *Polymer* **2001**, *42*, 7117.

(50) Lertwimolnun, W.; Vergnes, B. Influence of Compatibilizer and Processing Conditions on the Dispersion of Nanoclay in a Polypropylene Matrix. *Polymer* **2005**, *46*, 3462.

(51) Paul, D. R.; Robeson, L. M. Polymer Nanotechnology: Nanocomposites. *Polymer* **2008**, *49*, 3187.

(52) Dennis, H. R.; Hunter, D. L.; Chang, D.; Kim, S.; White, J. L.; Cho, J. W.; Paul, D. R. Effect of Melt Processing Conditions on the Extent of Exfoliation in Organoclay-Based Nanocomposites. *Polymer* **2001**, *42*, 9513.

(53) Leung, S. N.; Wong, A.; Guo, Q.; Park, C. B.; Zong, J. H. Change in the Critical Nucleation Radius and Its Impact on Cell Stability During Polymeric Foaming Process. *Chem. Eng. Sci.* **2009**, *64*, 4899.

(54) Bhattacharya, S. N.; Kamal, M. R.; Gupta, R. K. *Polymeric Nanocomposites: Theory and Practice*; Hanser Publishers: Cincinnati, OH, 2008.

(55) Mihai, M.; Huneault, M. A.; Favis, B. D. Crystallinity Development in Cellular Poly(lactic acid) in the Presence of Supercritical Carbon Dioxide. *J. Appl. Polym. Sci.* **2009**, *113*, 2920.

(56) Avella, M.; Cosco, S.; Volpe, G. D.; Errico, M. E. Crystallization Behavior and Properties of Exfoliated Isotactic Polypropylene/Organoclay Nanocomposites. *Adv. Polym. Technol.* **2005**, *24*, 132.

(57) Takada, M.; Tanigaki, M.; Ohshima, M. Effects of CO_2 on crystallization kinetics of polypropylene. *Polym. Eng. Sci.* **2001**, *41*, 1938.

(58) Lee, S. T. *Foam Extrusion: Principles and Practice*; Technomic: Lancaster, PA, 2000.

(59) Koronfield, J. A.; Kumaraswamy, G.; Issaian, A. M. Recent Advances in Understanding Flow Effects on Polymer Crystallization. *Ind. Eng. Chem. Res.* **2002**, *41*, 6383.

(60) Janeschitz-Kriegl, H.; Ratajsli, E.; Stadlbauer, M. Flow as an Effective Promotor of Nucleation in Polymer Melts: A Quantitative Evaluation. *Rheol. Acta* **2003**, *42*, 355.

(61) Alizadeh, A.; Sohn, S.; Quinn, J.; Marand, H. Influence of Structural and Topological Constraints on the Crystallization and Melting Behavior of Polymers. 1. Ethylene/1-Octene Copolymers. *Macromolecules* **1999**, *32*, 6221.

Received for review June 4, 2010
Revised manuscript received August 24, 2010
Accepted September 2, 2010

IE101225F